NASA TT F-8855

(NASA TT F-8855)

X64 35592

X64 15082

21 p

Code 5D

# t; AERODYNAMIC EFFECTS OF ROCKET JET EXPANSION

cat 02

BY

P. Carrière and M. Sirieix Apr. 1964 21 p refs

**Translation of:** [Effects aérodynamiques de l'éclatement d'un jet de fusée]
Jahrbuch 1961 der Wissenschaftlichen Gesellschaft für Luftfahrt E. V. p. 234-239.

Transl. from → into ENGLISH

(Berlin)

[redacted]

NATIONAL AERONAUTICS AND SPACE ADMINISTRATION
WASHINGTON, D.C. APRIL 1964

NASA TT F- 8855

1

FACILITY FORM 602

N 71-71320 (ACCESSION NUMBER) (THRU)

21 (PAGES) NONE (CODE)

(NASA CR OR TMX OR AD NUMBER) (CATEGORY)

Unc

# AERODYNAMIC EFFECTS OF ROCKET JET EXPANSION

P. Carrière* and M. Sirieix**, Paris


## SUMMARY

Important aerodynamic effects occur at high altitudes when jet expansion takes place. During climb the external flow separation point is first found at the rocket base, then it moves upstream as far as the nose. The calculation method here discussed results from the application of a previous theory [3] which makes it possible to solve any problem regarding the confluence of flows when the separation point is known. In the present case, the introduction of a criterion of separation of the external boundary layer, assumed to be laminar, provides the necessary supplementary condition to locate the separation and to define the pressure level in the region of stagnation.

The theoretical predictions thus established have been compared to experimental results by means of schlieren pictures obtained at Mach 7. Both models tested were supported on a hollow shaft and fed with compressed air at expansion ratios varying from 1 to 1000. The experiments show that the theory gives correct predictions for the initiation and development of external separation at expansion ratios $p_j/p_0 < 100$. But at higher ratios the theory does not indicate the very noticeable slowing down in the evolution of the separation point. The causes of this discrepancy are discussed.


## 1. INTRODUCTION

In the course of the ascending trajectory of a ballistic rocket /234 the rapid decrease in atmospheric pressure with altitude causes the internal jet to expand as it leaves the nozzle, so that the external

---

*Scientific Director of Aerodynamics, ONERA
**Chief, Research Department

[illegible] U.S. Government Agencies and U.S. Government Contractors only.

flow separates over a distance that increases as the flight proceeds.

At high altitudes, under the combined effects of an important decrease in the Reynolds number and a sharp increase in the Mach number, we can reasonably expect the external boundary layer to remain laminar; hence the interference effects will be considerably greater.

The primary object of the basic theoretical and experimental research into these phenomena, recently undertaken at ONERA, was to examine the extent to which theory [1, 2, 3] can, in simple cases, predict the appearance and development of flow separation due to jet expansion.

The initial results of this analysis are presented below.

## 2. SCOPE OF RESEARCH

In this preliminary study the experimental conditions were designed to create in the wind tunnel the effects likely to be observed during a flight characterized by strong interference, virtually necessitating a laminar external boundary layer.

In order to define more closely the region of simulation investigated, we shall first relate it to the possible trajectories of various types of ballistic rockets.

The interference effects produced depend on the power of the jet and the nature and state of the external boundary layer involved; they are, therefore, linked with the flight plan of the rocket and the characteristics of its propulsion system.

It may be assumed that the launching trajectories of various ballistic rockets (space vehicles, IRBM, etc.) are generally located in the corridor shown in the Mach number-altitude diagram of Figure 1.

Thus the altitude range of the experimental study which corresponds to Mach 7, lies between 38 and 57 km.

The parameter $p_j/p_0$ which, in the first analysis, characterizes the power of the jet, is simultaneously a function of the altitude $p_0$ and the characteristics of the propulsion system (chamber pressure $p_{ij}$, Mach number at nozzle exit $M_j$, chemical composition of combustion gases defining $\gamma_j$). An estimate of $p_j/p_0 = f(M_0)$, based on Fig. 1, was made for the following propulsion system characteristics:

$$p_{ij} = 35 \text{ bars}, \quad M_j = 3, \quad \gamma_j = 1.25.$$

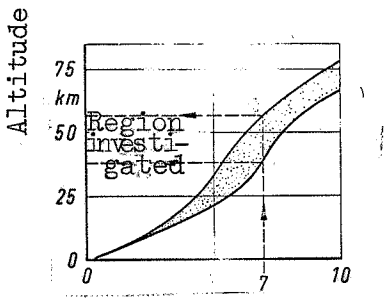


Fig. 1. Ballistic Rockets. Mach number vs. Altitude Region of Launching Trajectories.

The corresponding curve is shown in Figure 2. In this case at Mach 7 $p_j/p_0$ may vary between 200 and 2000 depending on the flight altitude. In the wind tunnel tests we achieved $p_j/p_0$ values ranging from 1 to 1000, which covers a large part of the flight region and enabled us to follow continuously the development of separation with $p_j/p_0$ from the moment it first appeared.

A final key factor is the nature and state of the external boundary layer which, in a first analysis, can be characterized by the Reynolds number $R_L$ referred to the total length of the rocket. The variation of this parameter in the course of the flight, derived from Figure 1, is shown in Figure 3 for an arbitrary length L = 10 meterss. Taking into account hypersonic transition conditions, this figure shows clearly that even for relatively large rockets, the external boundary layer will, in many cases, remain laminar, as soon as the Mach number reaches values of the order of 6 to 7. /235

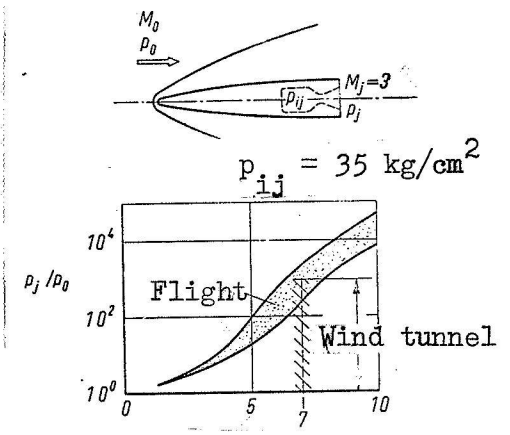


Fig. 2. Variation in Expansion Pressure Ratio $p_j/p_0$.

The range of Reynolds numbers with which we were able to experiment covers a large part of the flight corridor, at Mach 7.

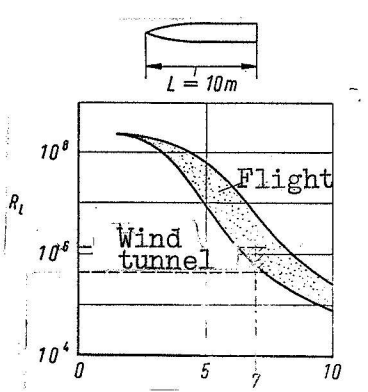


Fig. 3. Evolution of Reynolds Number in flight.

## 3. ANALYSIS OF THE SEPARATION EFFECT

The interaction of the internal and external flows can be analyzed for the simple case of a model with a conical head and a cylindrical body at a zero angle of attack (Figure 4). Let us examine the various aspects of the problem for a progressively increasing ratio $p_j/p_0$.

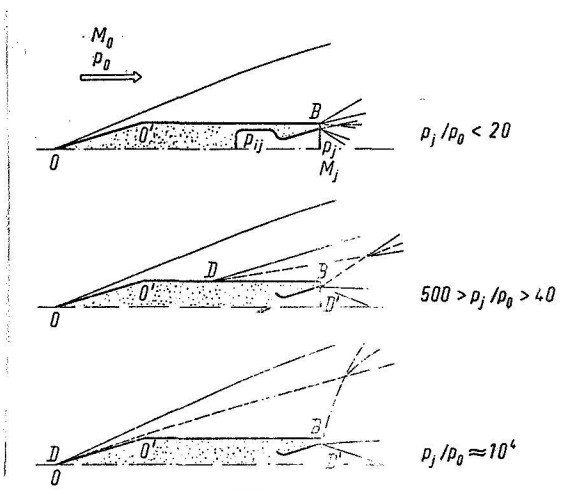


Fig. 4. Interaction of Internal and External Flows. Development of Separation as a Function of $p_j/p_0$.

At low values of $p_j/p_0$, the internal and external flows separate on either side of the base B and rejoin a short distance below B.

This region can be studied by the techniques proposed in [1, 2, 3]. An increase in $p_j/p_0$ leads to a point of separation D upstream from B. Under these conditions the plateau pressure level depends essentially on the state and nature of the boundary layer directly upstream from the point of separation [4].

The separation distance is closely linked with the conditions of the internal and external flows.

As the parameter $p_j/p_0$ continues to increase, the point D shifts upstream, reaching point 0' at a sufficiently high value $(p_j/p_0)_1$.

Thus, the point of separation is fixed, and the problem of determining the plateau pressure as a function of $p_j/p_0$ is theoretically identical with that of the initial case (base pressure).

This holds true as long as the pressure $p_1$ in the separation zone remains lower than the separation pressure over the nose cone.

When $p_1$ exceeds this value, the separation point moves rapidly from point 0' to point 0 (tip of nose cone), the entire surface of the rocket then being immersed in a separation zone.

The $p_j/p_0$ values indicated opposite each diagram in Figure 4 are intended to establish the order of magnitude of the various aspects of the phenomenon.

The theoretical problem now consists in determining the displacement of the point of separation as a function of $p_j/p_0$, as it moves from B to 0', with the following complementary hypotheses: boundary layers and mixing layers are laminar for the external flow and turbulent for the internal flow.

## 4. PRINCIPLE OF THE THEORETICAL CALCULATIONS

### 4.1 Review of Basic Concepts

Before examining the theoretical method of calculation, let us first review a few basic concepts which will be useful later on.

The flow pattern developing downstream from a separation point D at an arbitrary distance upstream from point B is shown in Figure 5. We shall assume that the Mach number $M_0$ upstream from D is uniform outside the boundary layer, the thickness of which $\delta_0$ is small. The generating conditions are $p_{i0}$ and $T_{i0}$.

In the same way the internal flow (generating conditions $p_{ij}$ and $T_{ij}$) is characterized in the nozzle exit plane by a Mach number

$M_j$ and a boundary layer thickness $\delta_j$.

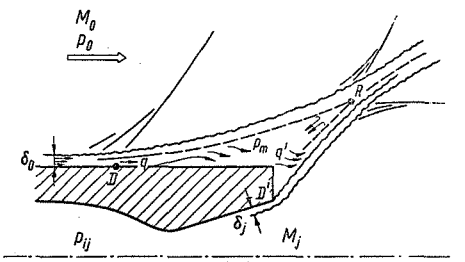


Fig. 5. Separation Due to Expansion of Jet. Real Flow.

After separating at D and D' each of the flows undergoes a process of isobaric mixing at the pressure $p_m$ in the presence of a stagnant zone.

On approaching the zone of confluence near R, the two jets respectively suffer a deflection $\Psi$ (external flow) and $\Psi'$ (internal flow), so that they flow in the same direction and at the same pressure.

Under the action of the corresponding recompression, part of the fluid circulating in each mixing layer flows back into the stagnant zone. Let q and q' be the respective contributions to this reflux of the external flow and jet.

An analysis of the problem [2, 3] has made it possible to establish a relation between the deflections $\Psi$ (or $\Psi'$) and the flows q (or q'), on the basis of the fundamental results obtained for laminar [5] and turbulent [6] conditions.

In each of these relations, which may be regarded as a criterion of confluence, there occurs the Mach number $M_1$ at the edge of the jet, /236 the ratio $T_m/T_i$ of the stagnant-zone temperature and the generating temperature, a dimensionless coefficient expressing the flow q, and a parameter characterizing the state of the initial boundary layer:

$$\begin{cases} \Psi = f\left[ M_1, \dfrac{T_m}{T_i}, \dfrac{q}{f_1 u_1 \overline{DR}\lambda}, (\delta_0) \right], \\ \\ \bar{\Psi} = f\left[ M'_1, \dfrac{T_m}{T_{ij}}, \dfrac{q'}{f'_1 u'_1 \overline{D'R}\lambda}, (\delta_j) \right]. \end{cases} \tag{1}$$

The Mach number $M_1$, established in the perfect fluid at the boundary of the external separation, is defined by the ratio $p_m/p$ of the stagnant zone and the pressure p of the unseparated flow, the corresponding Mach number M being known.

The ratio $p_m/p$ is also fixed by the separation conditions effective at point D [4].

## 4.2 Theoretical Solution

The flight conditions ($M_0$, $T_1$, $p_0$) being given, the external flow about the rocket is assumed known; it is proposed to calculate the value $p_{ij}$ of the generating pressure corresponding to separation at a specific point D. The solution is obtained by successive approximation:

We know (Figure 6):

x = distance from D to plane of base,

M = Mach number at D,

$c_f$ = coefficient of friction characterizing the laminar boundary layer at D in the absence of separation,

$M_j$ = Mach number at nozzle exit.

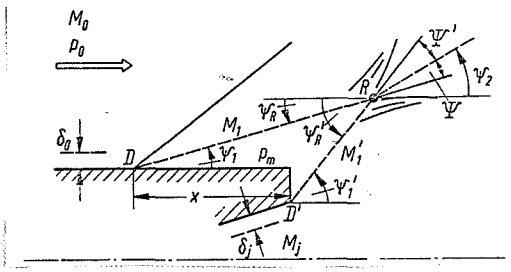


Fig. 6. Separation due to Expansion of Jet. Schematic.

Furthermore, we shall make the simplifying assumption that $T_m = T_{i0} = T_{ij}$.

The calculations then proceed as follows:

a) The criterion of laminar separation as defined in [4] gives us the pressure jump:

$$\frac{p_m}{p} = f\,(M,\ c_f) = 1 + 1.7\,M\sqrt{c_f}. \qquad (2)$$

b) The equations of oblique impact applied at D, starting from this compression ratio, gives us the Mach number $M_1$ and the initial direction $\nu_1$ of the separated streamline jets.

The method of characteristics then permits us to calculate the (generally curved) line of the jet DR.

c) We take an a priori value of $p_{ij}$, and hence of $p_j$, and calculate the isobaric line D'R, defined by the expansion pressure ratio $p_m/p_j$ starting from the nozzle exit conditions.

d) We now know the Mach numbers $M_1$, $M_1'$ and the directions of the two ideal jet lines just ahead of their point of confluence R. Finally, theory of a perfect fluid (oblique impact or adiabatic recompression) gives us the deflections $\Psi$ and $\Psi'$ of the two flows after confluence (same terminal direction and pressure).

e) As previously explained, the application of the angular criterion of recombination, starting from $\Psi$ and $\Psi'$, gives algebraic values of the components q and q' contributed to the stagnant zone by the two flows, and hence the value of q + q' attached to the a priori value of $p_j/p_0$. For the solution to be acceptable, we must have $q + q' = 0$. Otherwise, the calculations are repeated, starting from point C, for another value of $p_j/p_0$, etc. We thus get an element of a curve $q + q' = f(p_j)$, the ordinate of which at the origin $(q + q' = 0)$ leads to the solution $p_j$ of the problem.

Note. If the generating temperatures (or enthalpies) $T_{i0}$ and $T_{ij}$ of the two flows are different, it is clear that the stagnant-zone temperature $T_m$ establishes itself at an intermediate level which must be determined. Without entering into a detailed discussion of the calculations, we shall confine ourselves to indicating the principle involved: across each mixing zone, immediately upstream from the point of confluence, the generating enthalpy varies continuously from $H_m$ to $H_{i0}$ for the external flow and from $H_m$ to $H_{ij}$ for the jet. The fluid particles of each of these mixing layers converging at R in the stagnant zone, contribute enthalpy fluxes h (external flow) and h' (rocket jet).

The theory of recombination enables us to evaluate these fluxes in the form:

$$h = H\left(q, \frac{T_m}{T_{i0}}\right),$$

$$h' = H\left(q', \frac{T_m}{T_{ij}}\right).$$

Therefore, to generalize the initial method of calculation, we need only repeat operations c, d, e for different values of $T_m$ and $p_j$.

Each pair $(T_m, p_j)$ is thus associated with specific values of q, q', h, h'; the required solution corresponds to the simultaneous fulfillment of the conditions:

$$q + q' = 0,$$

$$h + h' = 0$$

corresponding to mass and thermal equilibrium of the stagnant zone.

## 5. EXPERIMENTAL VERIFICATION

### 5.1 Model, Experimental Setup

Two Chalais-Meudon hypersonic wind tunnels [7] were used for the experiments at Mach 7: the pilot tunnel $R_0$, diameter 130 mm, blast duration 4 seconds, and the tunnel $R_2$, a larger 300 mm diameter installation permitting experimentation at the highest expansion pressure ratios $p_j/p_0$ without blocking effects.

The generating conditions of the external flow, more or less the same for both installations, were as follows:

Pressure: $10 \text{ bars} \leqq p_{i0} \leqq 20 \text{ bars}$,

Temperature: $T_{i0} \approx 620^{\circ}K$,

Reynolds number of undisturbed flow $U_0/v_0$ varying correctively from 45,000 to 81,000 $cm^{-1}$.

To supply the model with compressed air without interference from a lateral support, the following arrangement was employed: /237

The test model was mounted on a hollow shaft. Compressed air, fed through this channel, was ejected parallel with the axis through an annular nozzle with a Mach number of 3 (Figure 7).

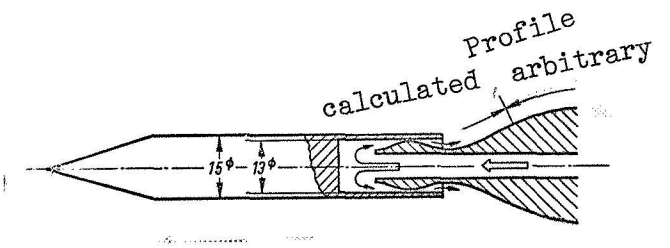


Fig. 7. Setup for Investigating Jet Expansion.
$M_j = 3$.

However, the outside diameter of the shaft represents a considerable proportion of that of the ejection nozzle.

To eliminate any effect of the central core on the free boundary of the internal flow under conditions of significant separation, the shaft was given the profile of the envelope of the real jet over a sufficient length (Figure 7).

The generating pressure $p_{ij}$ of the internal flow, which could be regulated from one blast to another, varied between 0.5 and 80 bars, the temperature generally differing little from that of the external flow $550^{\circ}K \leqq T_{i0} \leqq 800^{\circ}K$.

The two test models used in this preliminary study were cylindrical cones, 15 mm in outside diameter, with aspect ratios $\lambda = 6.66$ and 11, respectively. The half-angle at the apex of the cone was $1.5^{\circ}$.

## 5.2 Experimental Method

A picture of the development of separation as a function of the blast level was obtained by means of Schlieren photos of the flow (exposure time = 0.002 seconds, continuous illumination), some examples of which are shown in Figures 8 and 9.

A very careful preliminary adjustment of the model, both vertical and lateral, is required to obtain the strictest possible symmetry of separation; it was observed that minor angular variations

in position sometimes result in a relatively serious displacement of the origin of the effect on one side or other of the model.

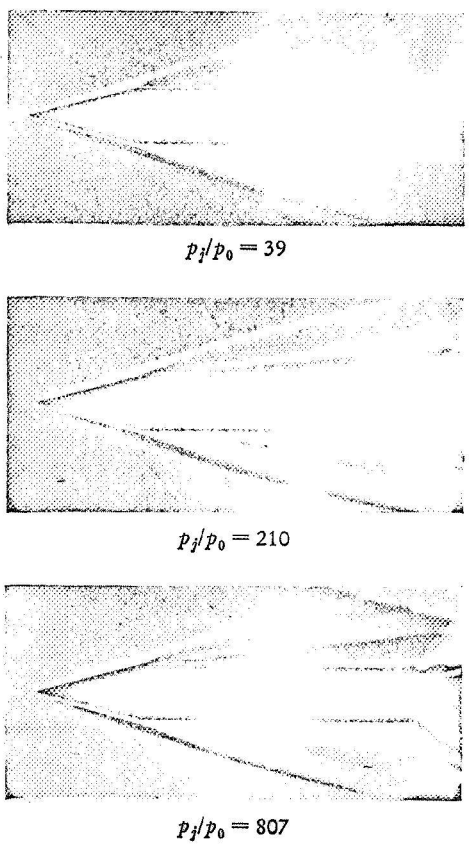


Fig. 8. Schlieren Pictures. Model $\Lambda = 6.66$, $M_0 = 7$.

Aside from the information it gives on the nature and state of the boundary and mixing layers, the schlieren method has proven itself to be a precise and convenient means of rapidly correcting slight errors in orientation.

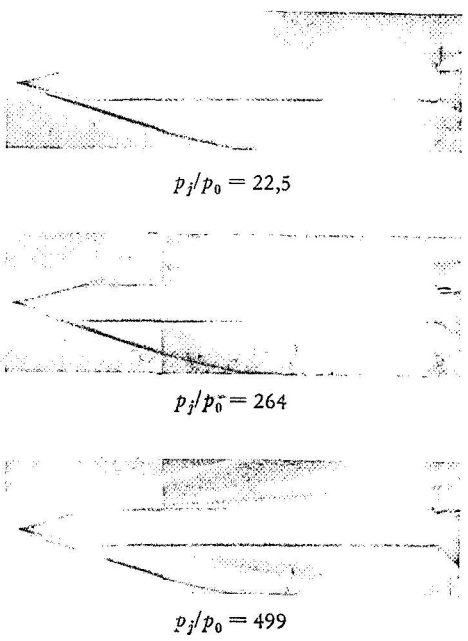


Fig. 9. Schlieren pictures. Model $\Lambda = 11$, $M_0 = 7$.

## 5.3 Analysis of Results

Determining the origin of separation from schlieren pictures, however, involves a certain element of arbitrariness. A careful inspection of Figures 8 and 9 shows quite clearly both the outside edge of the boundary layer [4], whether attached to the obstacle or separated from it, and the shock wave generated by the separation.

Because of their negligible curvature, these lines can be equated with straight lines without appreciable error.

The analysis shows that the contours of the boundary layer, of the separation, and of the shock wave it generates converge more or less in a common point, chosen provisionally as the origin of separation by analogy with the theoretical scheme.

Furthermore, schlieren photography confirms the laminar nature of the external flow up to the point of confluence with the

internal flow (Figure 8).

5.4 Presentation of Results

The variation of the relative separation length x/D is presented in Figure 10 as a function of $p_j/p_0$ for the model with $\lambda = 6.66$. /238

The experiments show that this variation is not uniform.

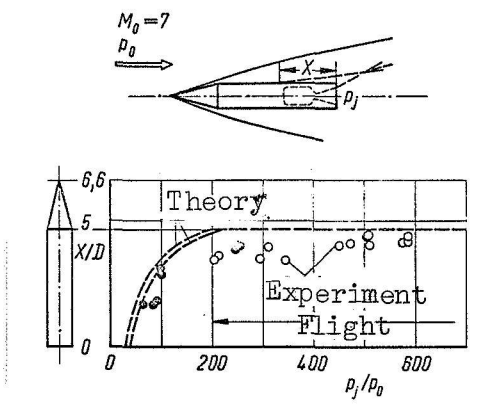


Fig. 10. Evolution of Separation, Model Cone-Cylinder. $\Lambda = 6.6$, $i = 0^\circ$.

| Theory | Experiment | Re/cm |
|---|---|---|
| Lower curve | ○ | 45 000 |
| Upper curve | ● | 81 000 |

In an initial phase, immediately after the appearance of separation, small variations in $p_j/p_0$ lead to an appreciable displacement of

the origin of separation ($p_j/p_0 < 100$).

At higher values of $p_j/p_0$, there is a distinct slowing down in the development of D.

The separation approaches the base of the cone more and more slowly as $p_j/p_0$ increases.

These test results also display a certain scatter; therefore they do not reveal an effect characterized by the experimental Reynolds number, which, moreover, according to (2) is only represented by its fourth root.

This scatter is largely attributable to fluctuations in the supply pressure of the rocket jet, which could not be completely eliminated in this experimental setup; it is very unlikely that it is due to an instability of the effect.

The theoretical curves shown in this graph were obtained by the method described in 4.2 assuming that $T_{ij}/T_{i0} = 1$.

To simplify the calculations the external separation boundary was established by the method of characteristics, neglecting the transverse nonuniformity of the external flow on the upstream face of the shock wave due to separation at D.

The appearance and development of separation in the initial phase of the phenomenon are satisfactorily predicted.

On the other hand, the theory does not represent sufficiently accurately the subsequent slowing down in the progress of the point D, which develops as $p_{ij}/p_0$ continues to rise.

For the model with $\lambda = 11$ (Figure 11) the general characteristics of the behavior of the point of separation are the same as the preceding example: a marked slowing down in the progress of the point D toward the base of the cone as $p_j/p_0$ increases; the scatter of the experimental results is the same.

In relation to this second series of results the predictions of the theory are somewhat less satisfactory for small values of $p_j/p_0$.

In both cases the present theory must be adjusted to improve the prediction for high values of $p_j/p_0$ corresponding to actual flight conditions, under which separation extends over a considerable part of the rocket fuselage.

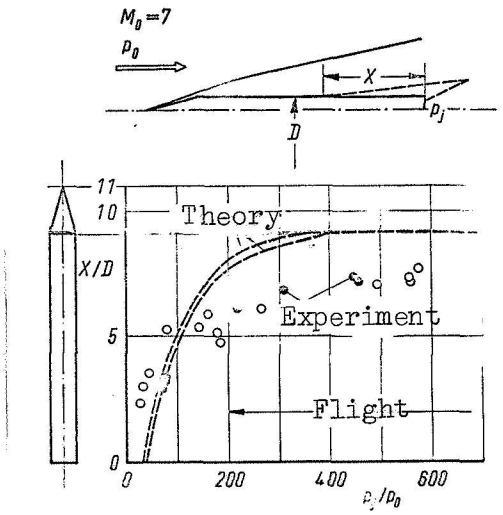


Fig. 11. Development of Separation, Model Cone-Cylinder. $\Lambda = 11$, $i = 0^{\circ}$.

| Theory | Experiment | Re/cm |
|---|---|---|
| Lower curve | ○ | 45 000 |
| Upper curve | ● | 81 000 |

## 6. CONCLUSION

The two examples presented here suffice to show the importance of a study of the separation problems involved in the hypersonic ascent of a ballistic rocket, at altitudes where the aerodynamic effects are still an important factor.

The initial appearance and development of separation can be predicted theoretically with sufficient precision in the initial phase; however, as the separation length increases, an appreciable gap develops between theory and experiment.

This discrepancy does not affect the principle of the theoretical scheme outlined here, but rather its present mode of application. Thus:

- the separation criterion employed has not yet been adequately verified at hypersonic speeds [4],

- the interaction between the boundary layer and the non-viscous flow has been neglected in calculating the local flow data upstream from the point of separation; now, a simple examination of the schlieren photos shows that here the thickness of the boundary layer is great enough to cause an appreciable modification of these data,

- the line of separation has been computed without taking into account the transverse nonuniformity of the flow on the upstream face of the separation shock wave. This simplification leads to the suppression of a factor representing the curvature of the line of the jet [3], the effect of which is the greater, the longer the separation length, since, in the last analysis, the angle of the two lines of the jet at their confluence is the decisive factor in the solution.

Further research on the laminar separation criterion in a hypersonic flow in the presence of thick boundary layers and improved calculating methods applicable to a perfect fluid are therefore indispensable if any progress is to be made in solving this problem. /239

The experimental analysis of the structure of the separation effect should be pursued by means of pressure probes, and measurements of the thermal fluxes at the wall and stagnant-zone temperatures as a function of the jet temperatures.

The extreme sensitivity of the phenomena to the attitude of the model underlines the importance of a theory that would predict, even approximately, the dynamic and thermal effects of an extensive and asymmetric separation as a function of the oscillation of the rocket.

## DISCUSSION

Engineer K. Kraemer (Göttingen): The theory is partly based on the mass flows q and q'. Their sum must vanish. What assumptions were made in calculating these mass flows?

P. Carrière: The determination of the exchange flows q and q' follows directly from the application of the angular criterion of recombination $\Psi$ ($M_1$, $T_m/T_i$, q, $\delta_0$), as pointed out in 4.1. This criterion

results from the theory of a laminar mixture for the external flow and the theory of a turbulent mixture for the internal flow, with the following assumptions:

- Isentropic recompression from $p_1$ to $p_2$ of the flow outside the mixing layer.

- Isentropic recompression from $p_1$ to $p_2$ of the viscous flow along the line of separation between the particles flowing downstream and those flowing back toward the stagnant zone.

K. Kraemer: In the wind tunnel measurements the Mach number of the external flow $M_1 = 7$ and the Mach number at the nozzle exit $M_j = 3$. With a rocket the velocity in the jet should be greater than the velocity of the external flow. Given the above-mentioned Mach numbers this can only be achieved if a hot jet (i.e., with a high speed of sound) is ejected. Was a hot jet or a cold one used in the experiments ?

P. Carrière: The experiments described, which were designed to test the accuracy of a theory, were carried out with air, the stagnation temperature of which was equal to 620°K, in the two flows.

It should be noted that under flight conditions, the discrepancy between the stagnation temperatures of the two fluids tends to cancel out towards Mach 8 and then to become inverted.

## BIBLIOGRAPHY

1. Carrière, P. Interaction de l'écoulement externe et de l'écoulement interne à la sortie d'un réacteur, aux vitesses transsoniques et supersoniques (Interaction of External and Internal Flows at a Reactor Exit at Trans-sonic and Supersonic Speeds) Compte Rendu des J. I. S. A. (May 1957).
2. Carrière, P. Effet d'une injection de fluide dans l'eau morte, sur les conditions de recollement d'un écoulement plan supersonique (Effect of Fluid Injection Into Stagnant Zone on the Confluence of a Plane Supersonic Flow) C. R. Acad. Sci. 251, pp. 2877-2879, (1960).

3. Carrière, P. & Sirieix, M. Facteurs d'influence de recollement d'un écoulement supersonique (Factors Affecting the Confluence of a Supersonic Flow) Paper read at the 10th Congress of Applied Mechanics, Stresa, 1960.
4. Michel, R. Conditions de décollement de la couche limite à grande altitude, aux vitesses hypersoniques (Conditions of Separation of Boundary Layer at High Altitudes and Hypersonic Speeds) Paper read at the Congress of the WGL, Freiburg 1961. Yearbook of WGL, pp. 244-253.
5. Chapman, D. R. A Theoretical Analysis of Heat Transfer in Regions of Separated Flow. NACA TN 3792 (1956).
6. Korst, H. H., Page, R., Childs, M. A Theory for Base Pressure in Transonic and Supersonic Flow. University of Illinois, ME TN 392-2 (1955).
7. Rebuffet, P. Souffleries hypersoniques de recherches de l'ONERA (Hypersonic Wind Tunnels used in ONERA Research Projects) Paper read at the 4th European Aeronautical Congress, Cologne 1960. 1960 Yearbook of WGL, pp. 134-149.

FARADAY TRANSLATIONS
15 PARK ROW
NEW YORK 38, N. Y.